

Flicker Noise Mitigation in Direct-Conversion Receivers for OFDM Systems

Surendra Boppana*, Masoud Sajadieh† and Hossein Alavi†

(surendra@ufl.edu, masoud.sajadieh@intel.com, hossein.alavi@intel.com)

Abstract— Direct-conversion receiver (DCR) architecture has received considerable attention recently owing to its portable architecture and superior performance in terms of power and cost over its super-heterodyne counterpart. Flicker noise is one of the major impairments which severely affects the performance of the system. In this work, we investigate the use of signal processing techniques in the mitigation of flicker noise in OFDM-based systems which employ DCR architecture. The statistical properties of flicker noise are exploited to develop adaptive signal processing algorithms that reduce the effect of flicker noise in DCRs. Results indicate that signal processing algorithms can provide significant performance gain under low SNR conditions.

I. INTRODUCTION

A major source of degradation in DCRs is flicker noise. Flicker noise is present in all electronic devices, and is produced due to a variety of physical phenomenon [1], [2]. Flicker noise has a power spectral density which is inversely proportional to frequency. Due to the nature of flicker noise, it is dominant at frequencies close to zero, and hence impacts the performance of DCRs. The coupling of the flicker noise with the received signal occurs after down-conversion to baseband. Since the root-mean squared (rms) power of the received signal is in the order of micro-volts, flicker noise comprises a substantial fraction of the signal power, which leads to large signal distortions. The effect of flicker noise can be reduced by at the device level by techniques such as correlated double sampling [3], edge-extended design [4], employing large gate area devices [2], [5], etc. However, its effect cannot be completely mitigated. Its effect is more pronounced in CMOS devices [6].

Flicker noise, also known as pink noise or $1/f$ noise is intrinsically present in all electronic devices. It is characterized by a power spectral density (PSD), $S_f(f)$, which is inversely proportional to the frequency f , i.e. $S_f(f) \propto \frac{1}{f}$, $f > 0$. There has been recent interest in the use of signal processing techniques in mitigation of non-linearities in DCRs. This is motivated by the strong push towards flexible and software configurable receiver architectures as more and more functionality of a DCR is performed in the baseband using digital signal processors. Adaptive signal processing algorithms have been proposed [8] to tackle the non-linearities in DCRs. In this work, we investigate the use of adaptive signal processing algorithms in mitigating the effect of flicker noise in DCRs. Although the algorithms considered in this work can be applied to any DCR architecture, we specifically address the DCR architectures that support OFDM systems such as WiFi and WiMAX. Instead of taking a mathematically rigorous

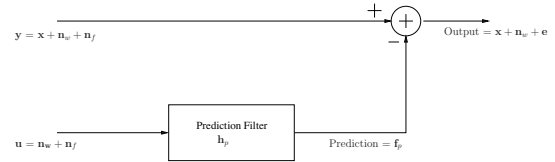


Fig. 1. Flicker noise mitigation through prediction filtering.

approach, we focus on key ideas and issues that impact the performance of the system.

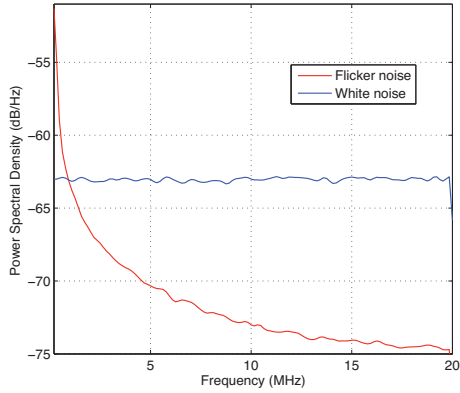
II. FLICKER NOISE MITIGATION IN OFDM-BASED SYSTEMS

In this section, we investigate the problem of flicker noise mitigation in DCRs in OFDM-based systems. We assume that flicker noise is the dominant source of impairment in the system, and other non-linearities such as dc offset, I/Q mismatch etc., have already been mitigated. For the sake of exposition, we first consider the case of optimal prediction of flicker noise assuming that the prediction filter has access to the “noise only” samples. This approach helps us in establishing bounds on the performance of practical filtering schemes, and in identifying the parameters that effect the performance of flicker noise mitigation algorithms. Later on, we discuss the practical issues involved in implementing the developed algorithms in DCRs designed for supporting OFDM-based systems. The modeling of flicker noise in this work is based on the results reported in [9], [10].

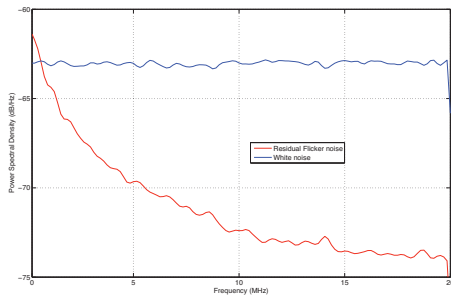
A. Optimal Prediction Filtering

The setup of the optimal prediction filtering scheme is shown in Fig. 1. The input signal $y(k)$ consists of the desired signal $x(k)$, which is assumed to be Gaussian, white noise $n_w(k)$, and flicker noise $n_f(k)$ all of which are pairwise independent. We also assume that the prediction filter \mathbf{h}_p has access to the present and all the past noise samples $u[k] = n_w[k] + n_f[k]$. Under this set-up, the optimal filter coefficients $h_p[n]$, $0 \leq n < L$ that minimize the mean square error between the noise samples \mathbf{u} and the predicted signal \mathbf{f}_p are given by the Wiener-Hopf equations [11].

The PSDs of the input signal $u(k)$, and the error signal $e(k) = u(k) - f_p(k)$ are shown in Figs. 2(a) and 2(b), respectively. The PSD of the flicker noise, and the white noise components of the input signal $u(k)$, are shown in Fig. 2(a). The corner frequency f_c , of the flicker noise is 1 MHz, the bandwidth of the system is 20 MHz, and the length of the



(a) PSD of flicker and white noise signals at input of prediction filter



(b) PSD of residual flicker and white noise signals

Fig. 2. PSD of the flicker and white noise signal before and after predictive cancellation, $f_c = 1$ MHz.

prediction filter is 50. We can observe in Fig. 2(a), the PSD curve of the flicker noise intersecting the PSD curve of the white noise at about 1 MHz. The flicker-to-thermal noise ratio is -2.7 dB.

Figure 2(b) depicts the PSD of the residual flicker noise and the white noise components after the subtraction of the predicted flicker noise sample $f_p(k)$ from the input signal $u(k)$ (The signal component, $x(k)$ is not shown in this figure). There are a few of interesting observations to be made. We note that the variance of the residual flicker noise is less than the variance of the input flicker noise component. This is not surprising, since the prediction filter exploits the high correlation among the flicker noise samples to predict the current flicker noise value, and cancel it out from the received signal. It is interesting to note that the PSD of the residual noise also follows the inverse power-law, where the PSD is proportional to $1/f^\alpha$, $\alpha < 1$.

The SNR gain due to mitigation of flicker noise through prediction filtering is plotted in Fig. 3 for several values of flicker noise corner frequencies, f_c . The input SNR is 10 dB, and is constant over all the corner frequencies simulated. The desired corner frequencies are simulated by appropriately scaling the variances of the flicker noise and white noise components. The SNR gain is defined as the ratio of the SNRs of the output signal $y_p(k) = y(k) - f_p(k)$ and the

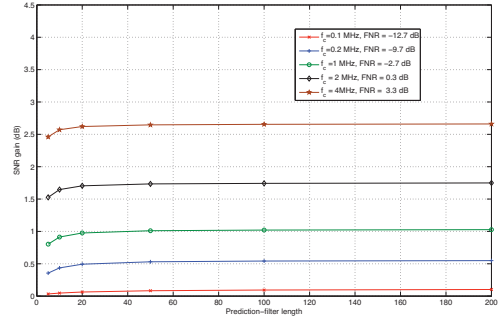


Fig. 3. SNR gain due to prediction filtering of flicker noise.

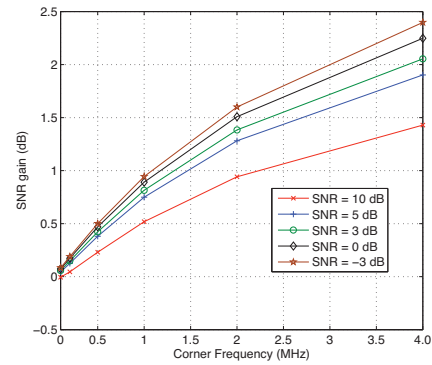


Fig. 4. SNR gain due to prediction filtering of data and noise signal.

received signal $y(k)$, i.e., $\text{SNR gain} = \frac{\sigma_w^2 + \sigma_f^2}{\sigma_w^2 + \sigma_e^2}$, where σ_e^2 is the variance of the residual flicker noise. Since the input to the prediction filter is “noise only” samples, the SNR gain due to prediction filtering is independent of the input SNR, and is dependent only on the corner frequency of the flicker noise (and FNR). From Fig. 3, we note that the SNR gain increases with an increase in the corner frequency. It can be seen from Fig. 3 that for any given corner frequency f_c , there is minimal improvement in performance for filter lengths greater than 50.

B. Modified Prediction Filtering

In this setup, the received signal $y(k)$ acts as the input to the prediction filter. The prediction filter generates an estimate $f_p(k)$, of the present sample of the flicker noise, and subtracts it from the received signal, $y(k)$. This design is motivated by the fact that under low SNR conditions, the received signal $y(k)$ is dominated by the flicker noise component $n_f(k)$, and $y(k)$ can provide a reasonable estimate of “noise only” samples. Since the input to the prediction filter consists of signal and noise components, the performance of the prediction filter strongly depends on the input SNR.

The SNR gain due to modified prediction filtering is shown in Fig. 4 for several values of input SNR, and flicker noise corner frequency f_c . For any given corner frequency, the SNR gain due to prediction filtering decreases as the input SNR increases. As the input SNR increases, the data component $x(k)$ increases, and affects the performance of the prediction

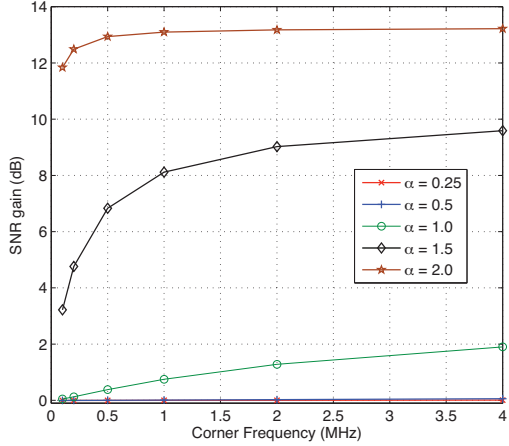


Fig. 5. SNR gain due to prediction filtering of flicker noise.

filter (In fact, the desired signal $x(k)$ behaves as white noise during the prediction of flicker noise). However at low input SNRs, there is considerable SNR gain achieved. For instance, when the input SNR is 3 dB, and the corner frequency of the flicker noise is 2 MHz, we observe an SNR gain of 1.35 dB.

Figure 5 depicts the SNR gain achieved due to modified prediction filtering of flicker noise for several values of the power-law exponent α . The input SNR is held constant at 3 dB, the corner frequency f_c of the flicker noise is 2 MHz, and FNR is 0 dB. We note that for a given value of corner frequency, SNR gain increases with an increase in α . Increase in α translates to increased correlation between the present and past samples, and an increase in correlation translates to better prediction of the current flicker noise sample.

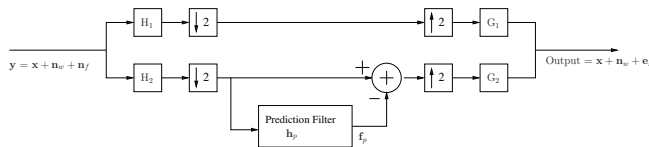


Fig. 6. Flicker noise mitigation through subband prediction filtering.

C. Sub-band Prediction Filtering

In the previous sections, we have considered the case of prediction filtering on the entire bandwidth of the system. However, due to the characteristics of the flicker noise, it is dominant only at frequencies close to dc, specifically, until the corner frequency, beyond which white noise is the dominant source of degradation. Based on this observation, we investigate prediction filtering schemes that operate in the band in which flicker noise is dominant, i.e. subband prediction filtering schemes. The prediction filtering mechanism of the subband filtering is quite similar to that of the modified prediction filtering of Section II-B, except that prediction filtering is performed on a low-pass filtered signal in which flicker noise is the dominant component. The setup of subband

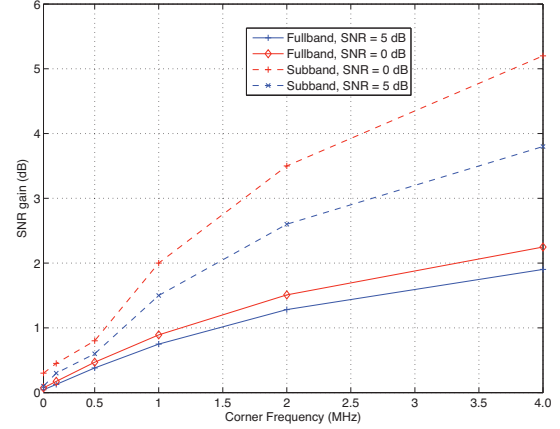


Fig. 7. SNR gain due to subband prediction filtering of data and noise signal.

prediction filtering is shown in Fig. 6. Analysis/Synthesis [12] filters are employed to decompose the input signal $y(k) = x(k) + n_w(k) + n_f(k)$ into multiple bands, and prediction filtering is performed on the band in which flicker noise is the most dominant noise source (this corresponds to the band of frequencies closest to dc). The number of analysis/synthesis sections is determined based on the input SNR, flicker noise corner frequency f_c , FNR, and the implementation complexity involved. The theory of analysis/synthesis filters is well developed, and there exists vast literature that deals with various aspects of the analysis/synthesis filters. In this work, we employ Quadrature Mirror Filter (QMF) banks [13] that result in perfect reconstruction of the input signal in the absence of the prediction filtering scheme. There exist a variety of techniques for the design of the QMF, and in this work we employ the design methodology described in [13].

The SNR gain due to sub-band prediction filtering of flicker noise is shown in Fig. 7, for several values of input SNR, and corner frequency f_c . The bandwidth of the system is 20 MHz. The number of analysis/synthesis sections were chosen such that the lowest subband contained all the frequencies from dc until f_c . For example, when the corner frequency $f_c=1$ MHz, we employ four analysis/synthesis filters on the received signal, and the prediction filtering is applied on the signal in band from dc until 1.25 MHz. Wiener filter of length 50 is employed to perform prediction filtering in the subband where flicker noise is the dominant source of noise. We observe that the SNR gain (measured over the entire signal bandwidth) is much greater in the case of subband prediction filtering than in the case of fullband prediction filtering. When $f_c=1$ MHz, and input SNR is 5 dB, the SNR gain due to subband prediction filtering is 1.5 dB compared to 0.8 dB of SNR gain in the case of fullband prediction filtering. The SNR gain is high when the input SNR is low, and the SNR gain decreases as the input SNR increases. This observation is similar to the behavior observed in the case of fullband prediction filtering described in Section II-B.

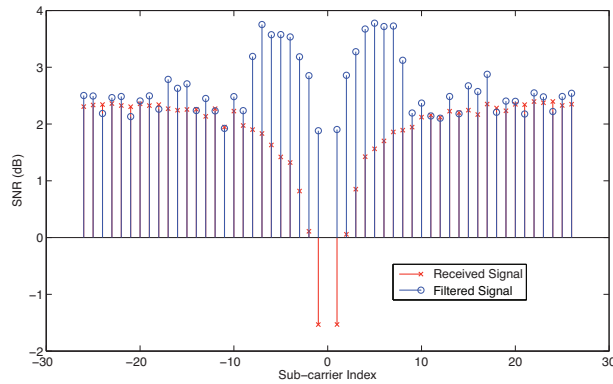


Fig. 8. Sub-band Prediction filtering of flicker noise, $f_c=2$ MHz

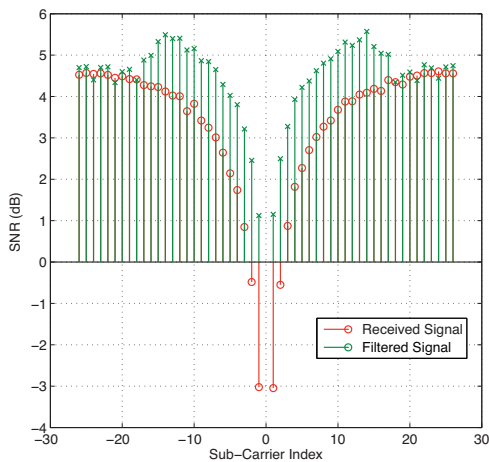


Fig. 9. Sub-band Wiener filtering of flicker noise, $f_c=2$ MHz

D. Flicker noise mitigation in OFDM systems

Until now, we have evaluated prediction filtering of flicker noise assuming that the transmitted signal, $x(k)$ is Gaussian. In this section, we evaluate the performance of prediction filtering (refer to Fig. 6) when the desired signal is an OFDM signal. We consider the case when the transmitted signal $x(k)$ is an OFDM signal generated based on the IEEE 802.11a standard. Due to the nature of the flicker noise, we expect the sub-carriers close to dc to be the worst affected. Figure 8 plot the SNR of the individual sub-carriers before and after subband prediction filtering for $f_c = 2$ MHz. The SNR of the input signal (measured over the entire band) is 0 dB. We observe that there is substantial SNR gain on the lower subcarriers. For instance, when $f_c=2$ MHz, the SNR gain for 1st subcarrier is about 4 dB. Note that the SNR gain decreases for the subcarriers that are located away from dc, which is not surprising considering the fact that the effect of flicker noise reduces as we move away from dc.

E. Flicker noise mitigation through Wiener filtering

In this section, we investigate the use of Wiener filtering in flicker noise removal.

The SNR gain due to subband Wiener filtering of flicker noise is shown in Fig. II-E for two different values of flicker noise. The input SNR of the signal (measured over the entire band) is 0 dB. When $f_c = 2$ MHz, we observe an SNR gain of 4.2 dB for subcarriers -1 and 1, and the SNR gain decreases as the sub-carrier index increases. The SNR gain achieved due to subband Wiener filtering is slightly greater than the gain achieved due to subband prediction filtering (refer to Fig. 8).

III. CONCLUSION

In this work, we investigated the use of adaptive filtering schemes in mitigating flicker noise in DCRs supporting OFDM systems. The strong correlation among the flicker noise samples can be exploited to perform prediction filtering of flicker noise, and the predicted signal subtracted from the received signal. However, we observed that this approach works only when the input SNR is low. Subband prediction filtering can be employed to improve the performance of prediction filtering. Substantial gains can be achieved when the flicker noise corner frequency is high. We also considered flicker noise mitigation through Wiener filtering of the received data in OFDM systems. We observed that subband Wiener filtering is superior to subband prediction filtering and can provide significant SNR gain on sub-carriers close to zero.

REFERENCES

- [1] K. K. Hung, P. K. Ko, C. Hu, and Y. C. Cheng, "A unified model for the flicker noise in metal-oxide-semiconductorfield-effect transistors," *Electron Devices, IEEE Transactions on*, vol. 37, no. 3, pp. 654–665, 1990.
- [2] E. Simoen and C. Claeys, "On the flicker noise in submicron silicon MOSFETs," *Solid State Electronics*, vol. 43, no. 5, pp. 865–882, 1999.
- [3] O. Oliaei, "Noise analysis of correlated double sampling SC integrators with a hold capacitor," *Circuits and Systems I: Fundamental Theory and Applications, IEEE Transactions on*, vol. 50, no. 9, pp. 1198–1202, 2003.
- [4] C. Y. Chan, Y. S. Lin, Y.C. Huang, S. S. H. Hsu, and Y. Z. Juang, "Edge-extended Design for Improved Flicker Noise Characteristics in 0.13-um RF NMOS," *Microwave Symposium, 2007. IEEE/MTT-S International*, pp. 441–444, 2007.
- [5] E. A. M. Klumperink, S. L. J. Gierkink, A. P. van der Wel, and B. Nauta, "Reducing MOSFET 1/f noise and power consumption by switched biasing," *Solid-State Circuits, IEEE Journal of*, vol. 35, no. 7, pp. 994–1001, 2000.
- [6] B. Razavi, "A study of phase noise in CMOS oscillators," *Solid-State Circuits, IEEE Journal of*, vol. 31, no. 3, pp. 331–343, 1996.
- [7] T. H. Lee, "The design of cmos radio-frequency integrated circuits, 2nd edition," *Communications Engineer*, vol. 2, no. 4, pp. 47–47, Aug.-Sept. 2004.
- [8] M. Cao, Y. Zheng, and H. K. Garg, "A novel algorithm for dc offsets and flicker noise cancellation in direct conversion receivers," *Communications Systems, 2004. ICCS 2004. The Ninth International Conference on*, pp. 441–445, 7-7 Sept. 2004.
- [9] F. N. Hooge, "1/f noise sources," *Electron Devices, IEEE Transactions on*, vol. 41, no. 11, pp. 1926–1935, Nov 1994.
- [10] N. J. Kasdin, "Discrete simulation of colored noise and stochastic processes and 1/f power law noise generation," *Proceedings of the IEEE*, vol. 83, no. 5, pp. 802–827, May 1995.
- [11] S. Haykin, *Adaptive filter theory (3rd ed.)*, Prentice-Hall, Inc., Upper Saddle River, NJ, USA, 1996.
- [12] P. P. Vaidyanathan, "Multirate digital filters, filter banks, polyphase networks, and applications: a tutorial," *Proceedings of the IEEE*, vol. 78, no. 1, pp. 56–93, 1990.
- [13] P. Vaidyanathan, "Quadrature mirror filter banks, m-band extensions and perfect-reconstruction techniques," *ASSP Magazine, IEEE*, vol. 4, no. 3, pp. 4–20, Jul. 1987.